

11. Amann, R. I., Krumholz, L. & Stahl, D. A. Fluorescent-oligonucleotide probing of whole cells for determinative, phylogenetic, and environmental studies in microbiology. *J. Bacteriol.* **172**, 762–770 (1990).
12. Porter, K. G. & Feig, Y. S. The use of DAPI for identifying and counting aquatic microflora. *Limnol. Oceanogr.* **25**, 943–948 (1980).
13. Bano, N. & Hollibaugh, J. T. Phylogenetic composition of bacterioplankton assemblages from the Arctic Ocean. *Appl. Environ. Microbiol.* **68**, 505–518 (2002).
14. Yager, P. L. *et al.* Dynamic bacterial and viral response to an algal bloom at subzero temperatures. *Limnol. Oceanogr.* **46**, 790–801 (2001).
15. Rochelle, P. A., *et al.* in *Nucleic Acids in the Environment* (eds Trevors, J. T. & van Elsland, J. D.) 219–239 (Springer, Berlin, 1995).
16. DeLong, E. F., Franks, D. G. & Alldredge, A. L. Phylogenetic diversity of aggregate-attached vs free-living marine bacterial assemblages. *Limnol. Oceanogr.* **38**, 924–934 (1993).
17. Rappé, M. S., Kemp, P. F. & Giovannoni, S. J. Phylogenetic diversity of marine coastal picoplankton 16S rRNA genes cloned from the continental shelf off Cape Hatteras, North Carolina. *Limnol. Oceanogr.* **42**, 811–826 (1997).
18. Fuhrman, J. A. & Davis, A. A. Widespread *Archaea* and novel *Bacteria* from the deep sea as shown by 16S rRNA gene sequences. *Mar. Ecol. Prog. Ser.* **150**, 275–285 (1997).
19. Bahr, M., Hobbie, J. E. & Sogin, M. L. Bacterial diversity in an arctic lake: a freshwater SAR11 cluster. *Aquat. Microb. Ecol.* **11**, 271–277 (1996).
20. Ducklow, H. in *Microbial Ecology of the Oceans* (ed. Kirchman, D. L.) 85–120 (Wiley, New York, 2000).
21. Davis, H. C. & Guillard, R. R. L. Relative value of ten genera of micro-organisms as food for oyster and clam larvae. *USFWS Fish Bull.* **58**, 293–304 (1958).
22. Glöckner, F. O. *et al.* An *in situ* hybridization protocol for detection and identification of planktonic bacteria. *System. Appl. Microbiol.* **19**, 403–406 (1996).
23. Hicks, R. E., Amann, R. I. & Stahl, D. A. Dual staining of natural bacterioplankton with 4',6-diamidino-2-phenylindole and fluorescent oligonucleotide probes targeting kingdom-level 16S rRNA sequences. *Appl. Environ. Microbiol.* **58**, 2158–2163 (1992).
24. Giovannoni, S. J., DeLong, E. F., Schmidt, T. M. & Pace, N. R. Tangential flow filtration and preliminary phylogenetic analysis of marine picoplankton. *Appl. Environ. Microbiol.* **56**, 2572–2575 (1990).
25. Garcia-Martínez, J. & Rodríguez-Valera, F. Microdiversity of uncultured marine prokaryotes: the SAR11 cluster and the marine *Archaea* of Group I. *Mol. Ecol.* **9**, 935–948 (2000).
26. Ludwig, W. *et al.* Bacterial phylogeny based on comparative sequence analysis. *Electrophoresis* **19**, 554–568 (1998).
27. Swofford, D. *PAUP\* 4.0* (Sinauer Associates, Sunderland, Massachusetts, 2000).

**Acknowledgements**

We thank R. Morris and C. Alexander for technical assistance; A. Soeldner and M. Nesson for electron microscopy expertise; W. Peterson, L. Feinberg and the US GLOBEC Program for CTD data; and the crew of the RV *Elakha*. This research was supported by Diversa Corporation and the National Science Foundation.

**Competing interests statement**

The authors declare that they have no competing financial interests.

Correspondence and requests for materials should be addressed to S.J.G. (e-mail: steve.giovannoni@orst.edu). The sequences have been deposited in GenBank under accession numbers AF510191 to AF510193.

**An unexpected specialization for horizontal disparity in primate primary visual cortex**

**B. G. Cumming**

Laboratory of Sensorimotor Research, National Eye Institute, National Institutes of Health, Bethesda, Maryland 20982, USA

The horizontal separation of the eyes means that objects nearer or farther than the fixation point project to different locations on the two retinæ, differing principally in their horizontal coordinates (horizontal binocular disparity). Disparity-selective neurons have generally been studied with disparities applied in only one direction<sup>1</sup> (often horizontal), which cannot determine whether the encoding is specialized for processing disparities along the horizontal axis. It is therefore unclear if disparity selectivity represents a specialization for naturally occurring disparities. I used random dot stereograms to study disparity-

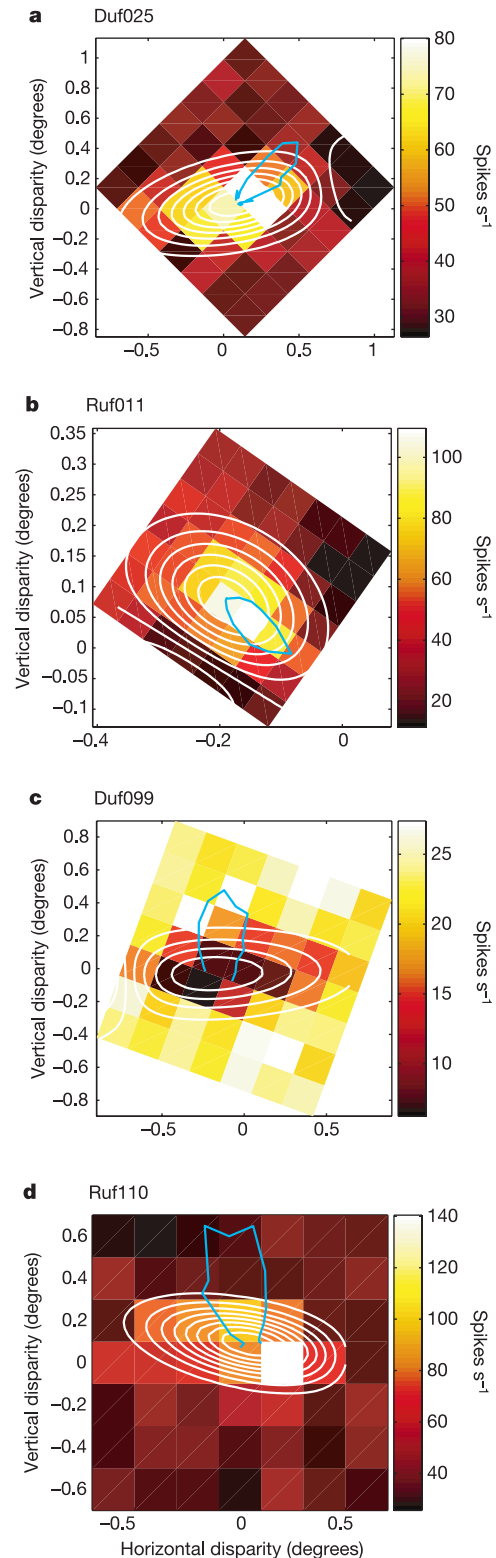


**Figure 1** Responses of four neurons to combinations of vertical and horizontal disparities. The white contour lines show the fitted two-dimensional Gabor function (see Methods). A polar plot of the monocular orientation tuning (stimuli spanning 180°) for each cell is superimposed (blue line, origin at the peak of the fitted Gabor). **a**, Despite an oblique orientation preference, cell 025 from monkey Duf (Duf025) produces a horizontally oriented disparity response. **b**, Ruf011 shows an obliquely oriented disparity response, matching the receptive-field orientation. **c**, **d**, Despite preferred orientations close to vertical, the disparity response surfaces for both Ruf110 and Duf099 are horizontally elongated. Duf099 illustrates a ‘tuned inhibitory’ response type. The s.e.m. for each data point was small relative to the mean (mean ratio 0.11).

selective neurons from the primary visual cortex (V1) of awake fixating monkeys. Many combinations of vertical and horizontal disparity were used, characterizing the surface of responses as a function of two-dimensional disparity. Here I report that the response surface usually showed elongation along the horizontal disparity axis, despite the isotropic stimulus. Thus these neurons modulated their firing rate over a wider range of horizontal disparity than vertical disparity. This demonstrates that disparity-selective cells are specialized for processing horizontal disparity, and that existing models<sup>2,3</sup> of disparity selectivity require substantial revision.

Points outside the fixation plane project to different locations on the two retinae. As the eyes are separated horizontally, these locations are related by a displacement along an axis very close to horizontal (horizontal disparity). There may also be a small vertical component<sup>4</sup>, but this is determined by eye position rather than the three-dimensional properties of the scene. Consequently, in central vision, the variation in disparity occurs along an axis that is very close to horizontal. Although there is a need for some information about vertical disparity to maintain alignment of the eyes and estimate viewing distance<sup>5</sup>, this does not require many finely spaced measures across the retina. Conversely, finely spaced measures of horizontal disparity are required to detect variations in depth within the scene.

It therefore seems natural to assume that neurons selective for binocular disparity encode horizontal disparities, but in principle they may signal disparities along other axes. Indeed, current understanding of the mechanism by which V1 receptive fields are constructed suggests that, depending on receptive-field orientation, different neurons signal disparities along different axes<sup>1,6</sup>. However, disparity-selective neurons have generally been tested with disparities applied along only one axis, which cannot reveal whether or not the neuronal responses are specialized to exploit the horizontal bias of naturally occurring disparities. In order to do this, it is necessary to explore responses of single neurons to disparities applied along several axes, using a visual stimulus that is isotropic (such as random dot stereograms, RDS).

Sixty disparity-selective neurons from V1 of two awake fixating monkeys were stimulated with combinations of vertical and horizontal disparity in RDS. Example responses are shown in Fig. 1. In all cases, large horizontal or vertical disparities yield a baseline firing rate, reflecting the response to uncorrelated dots within the receptive field. A set of disparity combinations elicited responses different from this baseline, occupying a region that was approximately elliptical. For most neurons, the long axis of this ellipse was near horizontal—they modulated their firing rate over a wider range of

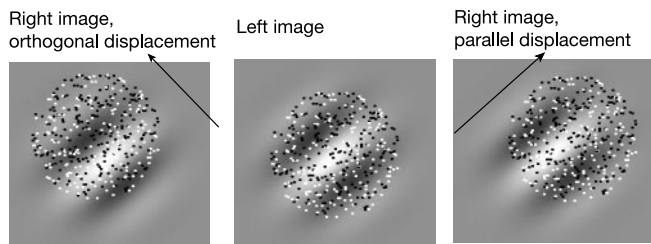
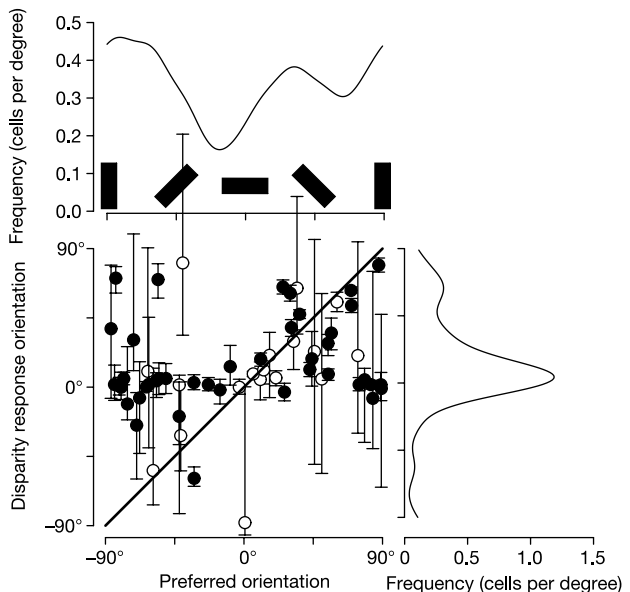


**Figure 2** Relationship between disparity tuning and receptive-field orientation, for simple models<sup>1</sup>. The receptive field (RF), depicted by the grey-level image, is selective for oblique contours. Superimposed is a random dot pattern like those used for the experiments (but this example has fewer dots, so that the RF is not obscured, and is smaller relative to the RF). Displacement of the dot patch orthogonal to the RF (left) should produce a stronger change in activity than a similar displacement parallel to the RF (right). The orientation of the disparity response surface should therefore match the monocular preferred orientation.

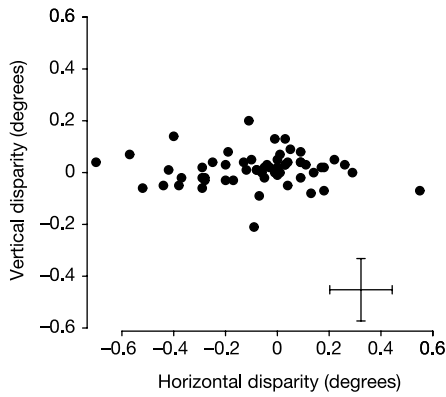
horizontal disparities than vertical disparities.

Figure 1b illustrates a less common pattern, where the response surface is not oriented horizontally. This might readily be explained by the properties of the monocular receptive field, as V1 neurons stimulated with extended contours show selectivity for the axis of orientation. If disparity selectivity is generated after this orientation-selective stage, simple models (like the binocular energy model<sup>2,3</sup>) predict a correlation between monocular orientation preference and the orientation of the disparity response surface (Fig. 2). If the orientation selectivity is the result of an oriented linear filter applied to the image, any simple disparity measure (for example, cross-correlation between the filtered images) applied after the filter will reflect the filter orientation. To examine this relationship, the monocular orientation preference of each neuron was measured independently with sinusoidal luminance gratings. Figure 3 compares preferred (monocular) orientation with the orientation of the disparity tuning surface for each neuron. Many points lie close to the identity line, in accordance with simple models. However, the majority show a near horizontal orientation of their disparity tuned responses, regardless of the monocular preferred orientation. This bias is highly significant ( $P \ll 0.001$ , Rayleigh test), and is so strong that it obscures any correlation between preferred orientation and the orientation of the disparity responses across the population (T-monotone association 0.004,  $P > 0.1$ ).

These horizontally oriented response surfaces represent a specialization for horizontal disparity in the sense that these neurons modulate their responses over a wider range of horizontal disparities than vertical disparities. The ability of the population to encode disparity also depends on differences between neurons, which could enable the population to encode a larger range than any individual



**Figure 3** Orientation of the disparity tuned response as a function of monocular orientation preference (dominant eye). Bottom scatter-plot for 60 neurons (32 from monkey Duf, 28 from monkey Ruf). Error bars show 95% confidence intervals. The orientation of the disparity response surface tends to be near zero (horizontal), regardless of the monocular orientation preference. Data points for neurons in which the two orientations are significantly different ( $P < 0.05$ , by resampling) are filled. The diagonal line shows the identity function. Each datum here is based on a mean of 845 stimulus presentations. The smoothed frequency distribution on the right shows a strong peak very close to zero (at 4°). Top, the frequency distribution for monocular orientations (above) shows a slight (but insignificant:  $P > 0.05$ , Rayleigh test) bias, which is away from zero.



**Figure 4** For each neuron, the preferred disparity identifies the disparity combination yielding the strongest response. The horizontal and vertical components of this preferred disparity are plotted here for each cell. The cross at the lower right shows the median value of the 95% confidence interval for each parameter. The horizontal components are more widely scattered than the vertical components, allowing the population to encode a wider range of horizontal disparities than vertical disparities.

neuron. The disparity that produced the strongest response was therefore examined for each neuron. This single point on the surface has horizontal and vertical disparity components. Differences between neurons in this preferred disparity were much greater for the horizontal than vertical components (Fig. 4, ratio of s.d.s 3.6,  $P \ll 0.001$ , *F*-test). A similar observation was made in one of the earliest studies of disparity tuning<sup>7</sup>, but a subsequent debate<sup>8,9</sup> raised doubts about its validity. However, all of these early studies used bar stimuli, where the orientation of the stimulus strongly influences the two-dimensional disparity tuning<sup>1</sup>. A few subsequent studies have used non-oriented stimuli<sup>10,11</sup>, but did not present data on

receptive-field orientation.

Both features of the data (the horizontal orientation of the disparity surface, and the greater horizontal scatter) indicate a specialization for encoding a wide range of horizontal disparities. The same features of the data make individual neurons, and the population as a whole, more sensitive to small changes in vertical than horizontal disparity (this can be appreciated from the spacing of the contour lines in Fig. 1). The remarkable finding is that neurons with different preferred orientation all exhibit the same anisotropy. A different anisotropy has been demonstrated in anaesthetized cats—vertically oriented simple cells show greater interocular differences in receptive-field structure (phase) than those with horizontal orientations<sup>12</sup>. I show here that the receptive-field orientation is not straightforwardly related to the direction of disparity encoding, so further work is required to understand the relationship between such monocular measures of receptive-field structure and disparity selectivity.

Considerable revision to the previously very successful energy model of disparity selectivity<sup>3</sup> will be required to explain these data. One possibility is that end- or side-stopping<sup>13</sup> precedes binocular combination, and hence partially determines the shape of the disparity-tuned response. (End-stopping might then prevent a neuron with a vertically oriented receptive field from responding to large vertical disparities.) An alternative is that these responses are constructed from many binocular subunits, differing from one another in their horizontal position disparity, but all having similar vertical position disparities. If the differences are large enough, the oriented structure of individual subunits can be obscured in the sum of all subunits. Although earlier observations also indicated a need to modify the model<sup>1,4–16</sup>, none of those required such an extreme revision.

Both the properties of single neurons, and the differences between neurons in the population, serve to maximize the range of horizontal disparities encoded by disparity-selective neurons in V1. This demonstrates that the properties of these neurons reflect

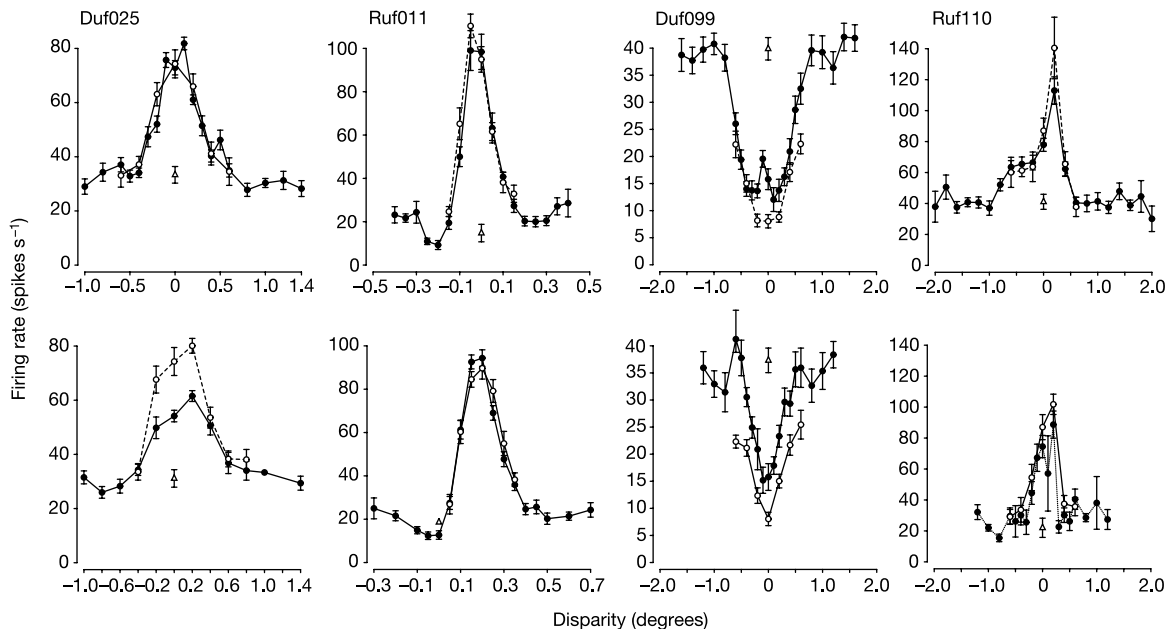


**Figure 5** In order to select the disparity combinations used, a wide range of disparities were first explored along each of two axes (solid symbols). These axes were orthogonal to the receptive field (RF; top row) or parallel to the RF (bottom row). Each open triangle shows the response to binocularly uncorrelated dots. The open circles show the

comparable rows of data extracted from the surface plots in Fig. 1, for comparison. As these trials were not interleaved, there are sometimes differences in the absolute response rates. Nonetheless, it is clear that the response surfaces in Fig. 1 cover the important range of disparities for these neurons.

the anisotropy of naturally occurring disparities. In the light of recent evidence indicating that activity in V1 disparity-selective neurons does not directly support stereopsis<sup>14,17–19</sup>, it is especially important to know if they show any specialization that is suited to a role in depth perception. The present study provides the strongest such evidence to date. □

Methods

Overview

A detailed description of the general methods has been published elsewhere<sup>17,20</sup>. Briefly, extracellular single-unit recordings were made in the primary visual cortex of two alert monkeys (*Macaca mulatta*), trained to maintain fixation with both eyes. Stimuli were presented on two EIZO Flexscan F980 monitors (mean luminance 41.1 cd m<sup>-2</sup>, contrast 99%), viewed via a mirror haploscope. The viewing distance was 89 cm, where each pixel subtended 0.019°. The positions of both eyes, along with the spike waveforms, were stored to disk for subsequent analysis. All protocols were approved by the Institute Animal Care and Use Committee, and complied with Public Health Service policy on the humane care and use of laboratory animals.

Experimental details

Stimuli were generated on a Silicon Graphics Octane workstation. Sinusoidal luminance gratings presented monocularly to each eye were used to determine the preferred orientation, spatial frequency, and minimum response field (MRF) of each neuron. Quantitative determination of the preferred orientation used a gaussian fit to data from at least nine orientations spanning 180°. MRFs were located at eccentricities between 2° and 9°. Dynamic RDS (generally 3° diameter) were centred over the MRF. Disparity-selective neurons were then tested with combinations of vertical and horizontal disparity, producing disparity displacements both parallel to and orthogonal to the preferred orientation. At least 49 combinations (seven parallel times seven orthogonal) were used. Stimuli were presented for 400 ms, and repeated a minimum of 5 times each (mean 13 repetitions). The range of disparities applied was determined by first measuring responses to a wide range of disparities (usually 15 disparities spanning ±1.2°, but this range was extended if there was evident modulation at either extreme) applied along an axis orthogonal to the receptive-field orientation. A similar range was then tested along an axis parallel to the receptive field. (Significant tuning in these preliminary tests was a criterion for entry into the study). The two-dimensional grid was then chosen so as to cover the region with the strongest modulation. Figure 5 shows the relationship between these initial measures and those taken from the two-dimensional grid for the four cells illustrated in Fig. 1.

Data analysis

The mean firing rate as a function of the disparity combination,  $f(x,y)$ , was fitted with a single two-dimensional Gabor function:

$$f(x,y) = A \exp[(y - Y)^2 / 2\sigma_y^2] \exp[(x - X)^2 / 2\sigma_x^2] \cos[2\pi\omega(x - X) + \phi] + B$$

by nonlinear regression, where  $A$ ,  $\omega$  and  $\phi$  are the amplitude, spatial frequency and phase of the cosine component,  $\sigma_x$  and  $\sigma_y$  are the standard deviations in orthogonal directions,  $X$  and  $Y$  are position offsets and  $B$  is the baseline firing rate. The two variables  $x$  and  $y$  were related to the horizontal and vertical disparity displacements by a single rotation through an angle  $\theta$ , which was a free parameter in the fit. Simply using the fitted orientation of the Gabor function did not always correctly identify the orientation of the disparity surface. (When the surface is close to gaussian, two equivalent fits are possible in which the value of  $\theta$  differs by 90°. Note that the Gabor still provides an excellent description, as a gaussian is a form of Gabor.) The fitted Gabor was therefore used only as a description of the data, from which a preferred disparity and orientation were determined. The preferred disparity was defined as the point that produced the largest deviation from the response to binocularly uncorrelated dots (maximum interaction position<sup>20</sup>). This identifies the trough for TI cells, which are characterized by inhibition at the 'preferred' disparity. The half-width at half-height of this peak (or trough) was measured along the two cardinal axes. The orientation of the long axis defined the orientation of the response surface, where zero indicates that the long axis lies horizontally.

Several analyses were performed to examine the possibility that the horizontal orientation of disparity responses was the result of variability in the animals' horizontal vergence angle. All of these suggested that the phenomenon was not attributable to eye movements. For example, the s.d. of vergence (horizontal and vertical) was calculated for each set of trials used. The geometric mean ratio (0.91) was not significantly different from unity ( $t$ -test on log ratios). Note also that the broad distribution of preferred horizontal disparities (Fig. 4) cannot readily be explained on the basis of fluctuations in vergence state.

Received 4 March; accepted 10 June 2002; doi:10.1038/nature00909.

1. Cumming, B. G. & DeAngelis, G. C. The physiology of stereopsis. *Annu. Rev. Neurosci.* **24**, 203–238 (2001).
2. Ohzawa, I. Mechanisms of stereoscopic vision: the disparity energy model. *Curr. Opin. Biol.* **8**, 509–515 (1998).
3. Ohzawa, I., DeAngelis, G. C. & Freeman, R. D. Stereoscopic depth discrimination in the visual cortex: Neurons ideally suited as disparity detectors. *Science* **249**, 1037–1041 (1990).
4. Mayhew, J. & Longuet-Higgins, H. C. A computational model of binocular depth perception. *Nature* **297**, 376–378 (1982).
5. Howard, I. P. & Rogers, B. J. *Binocular Vision and Stereopsis* (Oxford Univ. Press, Oxford, 1995).

6. Anzai, A., Ohzawa, I. & Freeman, R. D. Neural mechanisms for processing binocular information II. Complex cells. *J. Neurophysiol.* **82**, 909–924 (1999).
7. Barlow, H. B., Blakemore, C. & Pettigrew, J. D. The neural mechanisms of binocular depth discrimination. *J. Physiol. (Lond.)* **193**, 327–342 (1967).
8. Joshua, D. E. & Bishop, P. O. Binocular single vision and depth discrimination: Receptive field disparities for central and peripheral vision and binocular interaction of peripheral single units in cat striate cortex. *Exp. Brain Res.* **10**, 389–416 (1970).
9. Heydt, R. v. d., Adorjani, C., Anny, P. H. & Baumgartner, G. Disparity sensitivity and receptive field incongruity of units in the cat striate cortex. *Exp. Brain Res.* **31**, 523–545 (1978).
10. Maunsell, J. H. R. & van Essen, D. C. Functional properties of neurons in middle temporal visual area of the macaque monkey. II. Binocular interactions and sensitivity to binocular disparity. *J. Neurophysiol.* **49**, 1148–1166 (1983).
11. Nieder, A. & Wagner, H. Encoding of both vertical and horizontal disparity in random-dot stereograms by Wulst neurons of awake barn owls. *Vis. Neurosci.* **18**, 541–547 (2001).
12. DeAngelis, G. C., Ohzawa, I. & Freeman, R. D. Depth is encoded in the visual cortex by a specialized receptive field structure. *Nature* **352**, 156–159 (1991).
13. Hubel, D. H. & Wiesel, T. N. Receptive fields and functional architecture of monkey striate cortex. *J. Physiol. (Lond.)* **195**, 215–243 (1968).
14. Cumming, B. G. & Parker, A. J. Responses of primary visual cortical neurons to binocular disparity without depth perception. *Nature* **389**, 280–283 (1997).
15. Ohzawa, I., DeAngelis, G. C. & Freeman, R. D. Encoding of binocular disparity by complex cells in the cat's visual cortex. *J. Neurophysiol.* **77**, 2879–2909 (1997).
16. Livingstone, M. S. & Tsao, D. Y. Receptive fields of disparity-selective neurons in macaque striate cortex. *Nature Neurosci.* **2**, 825–832 (1999).
17. Cumming, B. G. & Parker, A. J. Binocular neurons in V1 of awake monkeys are selective for absolute, not relative, disparity. *J. Neurosci.* **19**, 5602–5618 (1999).
18. Cumming, B. G. & Parker, A. J. Local disparity not perceived depth is signalled by binocular neurons in cortical area V1 of the macaque. *J. Neurosci.* **20**, 4758–4767 (2000).
19. Prince, S. J. D., Pinton, A. D., Cumming, B. G. & Parker, A. J. The precision of single neuron responses in cortical area V1 during stereoscopic depth judgements. *J. Neurosci.* **20**, 3387–3400 (2000).
20. Prince, S. J. D., Cumming, B. G. & Parker, A. J. Range and mechanism of horizontal disparity encoding in macaque V1. *J. Neurophysiol.* **87**, 209–221 (2002).

Competing interests statement

The authors declare that they have no competing financial interests.

Correspondence and requests for materials should be addressed to B.G.C. (e-mail: bgc@lsr.nei.nih.gov).

Wnt-11 activation of a non-canonical Wnt signalling pathway is required for cardiogenesis

Petra Pandur\*†, Matthias Läsche\*, Leonard M. Eisenberg‡ & Michael Kühl\*†

\* Abt Entwicklungsbiochemie, Junior group SFB 271, Universität Göttingen, Humboldtallee 23, D-37073 Göttingen, Germany

† Abt Biochemie, Universität Ulm, Albert-Einstein-Allee-11, D-89081 Ulm, Germany

‡ Department of Cell Biology and Anatomy, Medical University of South Carolina, Charleston, South Carolina 29425, USA

Formation of the vertebrate heart requires a complex interplay of several temporally regulated signalling cascades<sup>1</sup>. In *Xenopus laevis*, cardiac specification occurs during gastrulation and requires signals from the dorsal lip and underlying endoderm<sup>2</sup>. Among known *Xenopus* Wnt genes, only Wnt-11 shows a spatio-temporal pattern of expression that correlates with cardiac specification, which indicates that Wnt-11 may be involved in heart development<sup>3,4</sup>. Here we show, through loss- and gain-of-function experiments, that XWnt-11 is required for heart formation in *Xenopus* embryos and is sufficient to induce a contractile phenotype in embryonic explants. Treating the mouse embryonic carcinoma stem cell line P19 with murine Wnt-11 conditioned medium triggers cardiogenesis, which indicates that the function of Wnt-11 in heart development has been conserved in higher vertebrates. XWnt-11 mediates this effect by non-